Exploring morphological variations of a laser-induced water jet in temporal evolution:

formation of an air bubble enclosing a water drop

# Exploring morphological variations of a laser-induced water jet in temporal evolution: formation of an air bubble enclosing a water drop

**Ross C C Chen, Y T Yu, K W Su and Y F Chen**

Department of Electrophysics, National Chiao Tung University, Hsinchu, 30010, Taiwan

E-mail: yfchen@cc.nctu.edu.tw

## Abstract

We explore the spatio-temporal dynamics of a water jet that is generated by laser-induced water breakdown beneath a flat free surface. We find that morphological variations in the temporal evolution can be divided into three categories depending on the depth parameter $\gamma$, which is the ratio of the water-breakdown depth to the maximum bubble radius. For a depth parameter in the range $0.8 \leq \gamma \leq 1.03$, we observe an intriguing pattern formation in which an air bubble perfectly encloses a water drop through the process of the Plateau–Rayleigh instability.

S Online supplementary data available from stacks.iop.org/LP/23/116002/mmedia

(Some figures may appear in colour only in the online journal)

## 1. Introduction

Bubbles are ubiquitous in many conditions such as nonlinear oscillation, bubble luminescence, and the well-known influence of erosion damage on material surfaces [1–4]. One interesting topic in the field of bubble dynamics is the interaction between a bubble and a free surface [5–8]. Research on this topic has mainly focused on the motion, oscillation and toroidal evolution (jet impact) of a bubble interacting with a composite surface [5–8]. During the oscillation period of the bubble, an upward liquid jet is usually observed to eject from the free surface [5, 6]. Very recently, several structures of a liquid jet were observed from different curvatures of the free surface, such as a flat free surface [9–11], spherical surface [12] and cylindrical surface [13]. The approaches for generating the bubble and the liquid jet include chemical and nuclear explosions, spark discharge and pulsed laser focusing. The advantage of using a laser-induced liquid jet over other methods is reproducibility and controllability [9, 11, 13, 14]. The

laser-induced liquid jet has been studied in film-free laser printing [9], volcanology [15] and biology and medicine [16]. Recently, the dependence of the initial morphology on the dimensionless parameter $\gamma = D/R_{\max}$ has been studied experimentally in a laser-induced water jet, where $D$ is the depth beneath the free surface and $R_{\max}$ is the maximum bubble radius [11]. It was found that when the depth satisfies $0.6 \leq \gamma \leq 1.1$, the laser-induced water jet is composed of a thin jet and a crown-shaped water jet. However, an investigation of the transient dynamics of the laser-breakdown induced water jet has not been performed yet.

In this work, we systematically explore morphological changes in the temporal evolution of a water jet generated by laser-induced water breakdown. We find that the crown-shaped water jet closes in the time evolution and that it forms an air bubble to surround the initial thin jet for depth in the range $0.8 \leq \gamma \leq 1.03$. Through the process of the Plateau–Rayleigh instability [17, 18], the surrounded thin jet turns out to have the structure of an air bubble enclosing a water drop. Furthermore, we find that for $1.03 < \gamma < 1.1$,
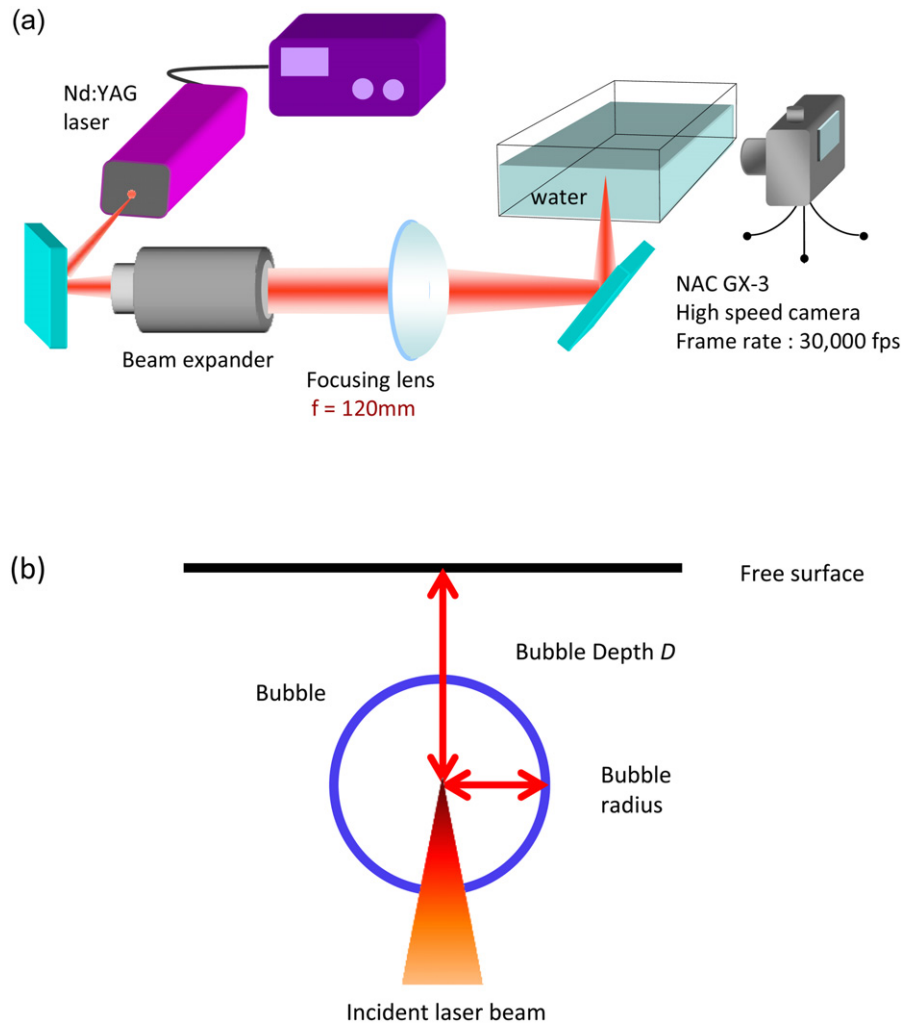
**Figure 1.** (a) Schematic diagram of the experimental setup. (b) Schematic diagram of the parameters of the bubble depth $D$ and the bubble radius.

only an air bubble can be formed in the final stage of the temporal evolution because the crown-shaped water jet is not high enough to enclose a sufficient amount of the thin jet. We finally find that for $0.6 < \gamma < 0.8$, the prior thin jet is usually bending and inclines to the sidewall of the crown-shaped jet.

## 2. Experimental setup

A schematic diagram of the experimental setup is shown in figure 1(a). A cavitation bubble is generated beneath a flat free surface by focusing a flash-pump pulsed laser (Nd:YAG, $\lambda = 1064$ nm) with a pulse width 6 ns from below a water tank vertically into tap water at room temperature (297 K) under atmospheric pressure. The energy of the laser beam after the mirror is around 16 mJ and the maximum radius of the bubble is about 1.25 mm. The dimension of the tank is $100 \times 70 \times 20$ mm$^3$ and the depth of the water is 13 mm for alleviating the influence of the bottom wall of the tank on the bubble. The water jet is reproducible and is recorded by a high-speed camera (NAC GX-3) with a frame rate of 30 000 fps and the exposure time is about 33 $\mu$s (unless otherwise specified). The bubble depth is defined in a dimensionless parameter

$\gamma = D/R_{\text{max}}$, where $D$ is the bubble depth beneath the free surface and $R_{\text{max}}$ is the maximum bubble radius, as depicted in the schematic picture of figure 1(b). In our previous studies [11], we observed that a thin jet was initially generated in laser-induced breakdown and subsequently a thick jet with a crown-shaped cup was created. The mechanism of crown formation is an interesting topic. It is speculated that perhaps the crown arises from the shock wave that is generated by the collapsing bubble below the water surface. However, in the experimental observation, we found that the crown-like structure is intimately correlated with the collapse of the water surface depression. In order to clarify this phenomenon, the laser was focused horizontally from the sidewall of a water tank into the water and the water jet was generated. Figure 2(a) depicts the evolution of the water jet in the time interval between 0 and 266 $\mu$s with a frame rate and shutter speed of 30 000 and 10 $\mu$s, respectively. It can be seen that during the first expansion of the bubble, a spike-shaped water jet is extruded and continually grows up; subsequently, the pressure in the bubble is decreased due to the expansion of the cavity. Then the bubble starts to collapse and move downward. Figure 2(b) shows more detailed images in the time interval
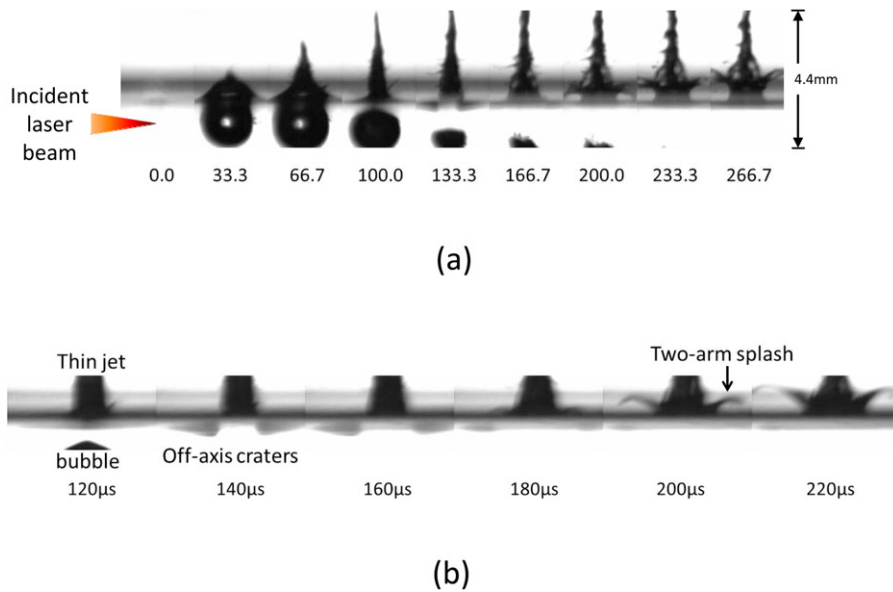
**Figure 2.** (a) A water jet generated by horizontally focusing the laser beam beneath the free surface. The frame rate is 30 kHz and the shutter speed is 10 $\mu$s. The time (in $\mu$s) is indicated at the bottom of each frame. (b) Detailed images for showing the surface depression. The frame rate is 50 kHz and the shutter speed is 3 $\mu$s. The time (in $\mu$s) is indicated at the bottom of each frame.

between 120 and 220 $\mu$s for clearly displaying the surface depression. As seen in the second picture of figure 2(b), the dynamics of the bubble cause the water surface to have a dramatic curvature change and then develop to a crater structure around the bottom of the thin jet. Intriguingly, it is found in the fifth picture of figure 2(b) that the recovery of the crater structure results in a two-arm outward splash beside the thin jet. The observation of the crater structure is similar to that of the crown-like structure in the vertical excitation shown in figure 1. In brief, the mechanism of crown formation is confirmed to be mainly related to the water surface depression. This mechanism is different from crown formation by the impact of a falling object on the water surface, where the water is pushed outward by the falling object, and then the surrounding water is splashed upward to form the crown [19]. In the following, we will focus on exploring morphological changes between the thin jet and the crown-shaped cup in the temporal evolution.

## 3. Results and discussion

Figure 3 shows a typical experimental result for morphological variations in the temporal evolution of the water jet generated by laser-induced breakdown at a depth of $\gamma = 0.9$. The crown-shaped structure can be seen to be an almost circular cup with a velocity approximately 6.2 m s$^{-1}$. As seen in the fourth row of figure 3, the crown-shaped water jet is closing and forms an air bubble to surround the prior thin jet. The closing motion of the crown-shaped water jet is analogous to the process of a flower closing its petals. The contraction of the crown-shaped liquid jet arises from two major forces: surface tension and under-pressure caused by air flow through the motion of the thin jet. Such an under-pressure phenomenon is known as the Bernoulli effect,

which has been confirmed to explain well the contraction of a crown-like water plume in laser ablation [20] and the closing motion of the splash and fluid after high-speed water entry [21, 22]. In the process of laser ablation or high-speed water entry, the instantaneous impact on the water surface usually generates a cavity with extremely low air density; consequently, the air flow around the cavity can cause the under-pressure phenomenon. However, in the present case the air density inside the crown does not significantly decrease; therefore, the Bernoulli effect is not as significant as in the process of high-speed water entry.

Just after the closing motion, the top rim of the cup-shaped jet pinches the prior thin jet into two segments to form an air bubble with a vertically elongated shape. In other words, the circular wall of the crown-shaped jet turns into the boundary of the air bubble and the enclosing segment of the prior thin jet develops into the central pillar of the air bubble. Shortly afterwards, the elongated shape of the air bubble starts to become a near spherical shape owing to the surface tension. The time interval from the pinch-off of the thin jet to the deformation of the air bubble is approximately 600–700 $\mu$s. During the shrinking of the air bubble, the top of the thick jet shows a ripple with a wavelength of about 0.27 mm on its surface. This ripple may be associated with the pinch speed of the crown wall. Moreover, the water pillar separates from the air bubble and finally shrinks into a drop of water with diameter about 0.33 mm, as shown in the last row of figure 3. The breakup of the water pillar into the waving structure to form smaller droplet, referred to as the Plateau–Rayleigh instability [17, 18], is rich with varieties of phenomena and applications [23]. A well-known example related to the Plateau–Rayleigh instability is the formation of small droplets when water is dripping from a faucet. Interestingly, the final water drop keeps moving upward and bounces between the top and bottom walls of the air bubble.
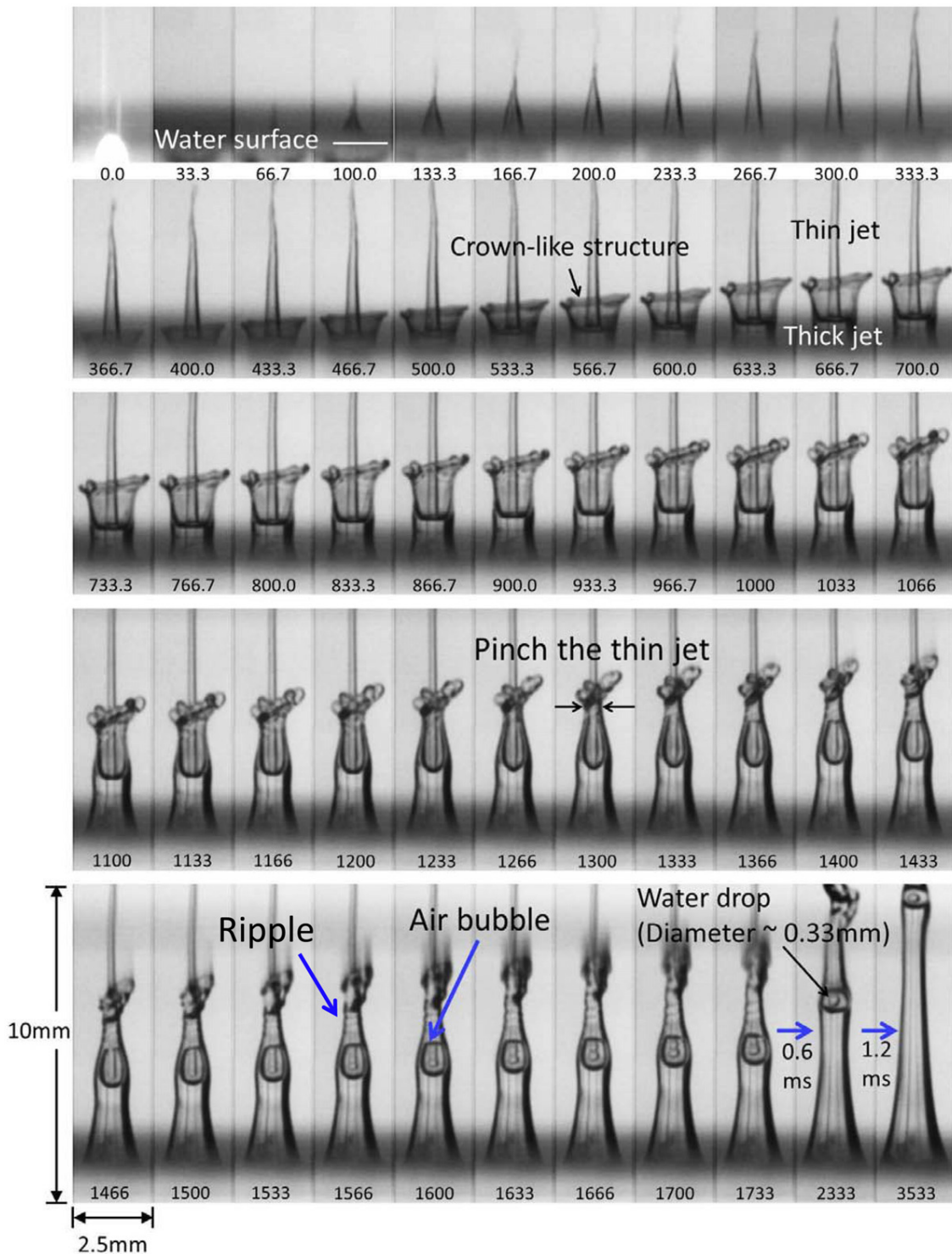
**Figure 3.** A typical experimental result for morphological variations in the temporal evolution of the water jet generated by laser-induced breakdown at a depth of $\gamma = 0.9$. The frame rate is 30 kHz and the time (in $\mu$s) is indicated at the bottom of each frame.

Eventually, the water drop stays on the bottom wall of the air bubble and is stably dragged up by the air bubble, as shown in the last picture of figure 3. The comprehensive evolution of the water jet can be seen from the supplementary material[1] for the movie corresponding to figure 3.

[1] See supplementary material (available at stacks.iop.org/LP/23/116002/ mmedia) for movie 1 corresponding to the results shown in figure 3.

Morphological variations of the water jet in the temporal evolution are significantly dependent on the depth of the cavitation bubble. The scenario shown in figure 3 for displaying an air bubble enclosing a water drop generally occurs for depth in the range $0.8 \leq \gamma \leq 1.03$. There are two other types of morphological changes of water jets generated at depths of $0.6 < \gamma < 0.8$ and $1.03 < \gamma < 1.1$, respectively. Figure 4 shows a typical result of the temporal evolution of the
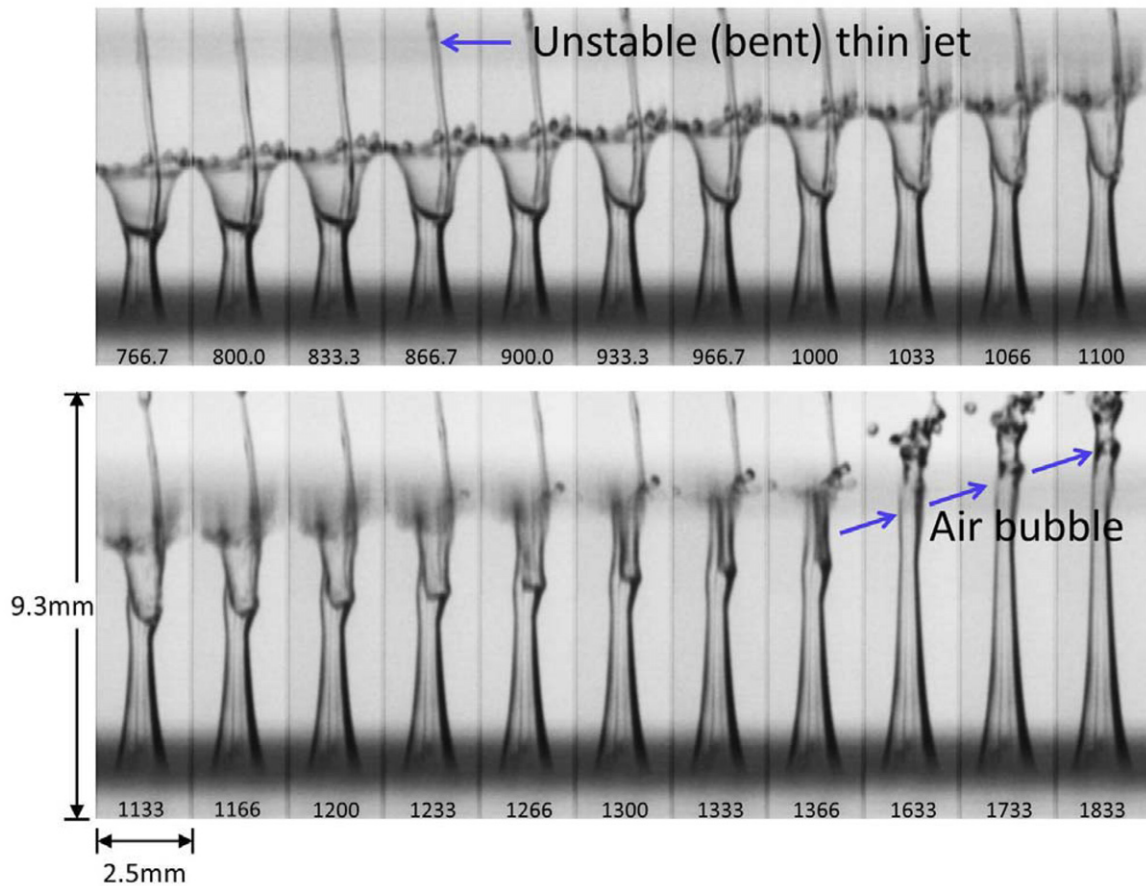
**Figure 4.** A typical result for morphological variations in the temporal evolution of the water jet generated at a depth of $\gamma = 0.7$. The frame rate is 30 kHz and the time (in $\mu$s) is indicated at the bottom of each frame.

water jet generated at a depth of $\gamma = 0.7$. In the early stages, the volume of the crown-shaped water jet can be seen to grow considerably. One might naturally expect that a stretched air bubble could enclose the prior thin jet to display a similar phenomenon as shown in figure 3. However, the thin jet is usually bending owing to the fact that the push force from the expanding bubble becomes overly strong. The bent thin jet generally inclines to the sidewall of the crown-shaped jet. Therefore, only an air bubble without any water drop can be formed in the final stages. The bubble is elongated because the ejected speed of the water jet becomes faster for a smaller $\gamma$ value. The comprehensive evolution can be seen from the supplementary material[2] for the movie corresponding to figure 4. On the other hand, for depth in the range $1.03 < \gamma < 1.1$, the wall of the crown-shaped water jet is not high enough to enclose the thin jet and thus there is no water drop inside the air bubble. Figure 5 shows morphological variations of the water jet at a depth of $\gamma = 1.04$. When the bubble depth is increased, the thick jet becomes wider and the air bubble turns out to be flatter. The comprehensive evolution can be seen from the supplementary material[3] for

the movie corresponding to figure 5. Note that for $\gamma < 0.8$ the ripple phenomenon shown in figure 3 is difficult to observe because the pinch speed of the crown wall is very fast. For $\gamma > 1.03$, the pinch of the crown wall perhaps does not induce a sufficient force to generate ripples.

As shown in figure 3, there are two breakup events for the water pillar separating from the air bubble to generate a water drop: the breakup times at the top and bottom ends of the water pillar. The result in figure 3 reveals that the breakup at the bottom end is approximately 130 $\mu$s earlier than the top end of the water pillar. We further measure the time difference $\Delta t = t_1 - t_2$ as a function of the parameter $\gamma$, where $t_1$ and $t_2$ are the breakup times for the top and bottom ends of the water pillar, respectively. Figure 6 shows the experimental result for the time difference $\Delta t$ in the range $0.8 \leq \gamma \leq 1.03$. The positive value of $\Delta t$ indicates that the breakup at the top end is later than the breakup at the bottom end. Furthermore, the value of $\Delta t$ increases with increasing depth parameter $\gamma$. Since the height of the crown wall is not high enough for $\gamma > 1.03$, the top end of the water pillar does not break up but mixes into the top wall of the air bubble. For $\gamma < 0.8$, the breakup events cannot be observed because the thin jet is bending.

Based on thorough experimental observations, the dependence of the pinched altitude $H$ of the crown-shaped
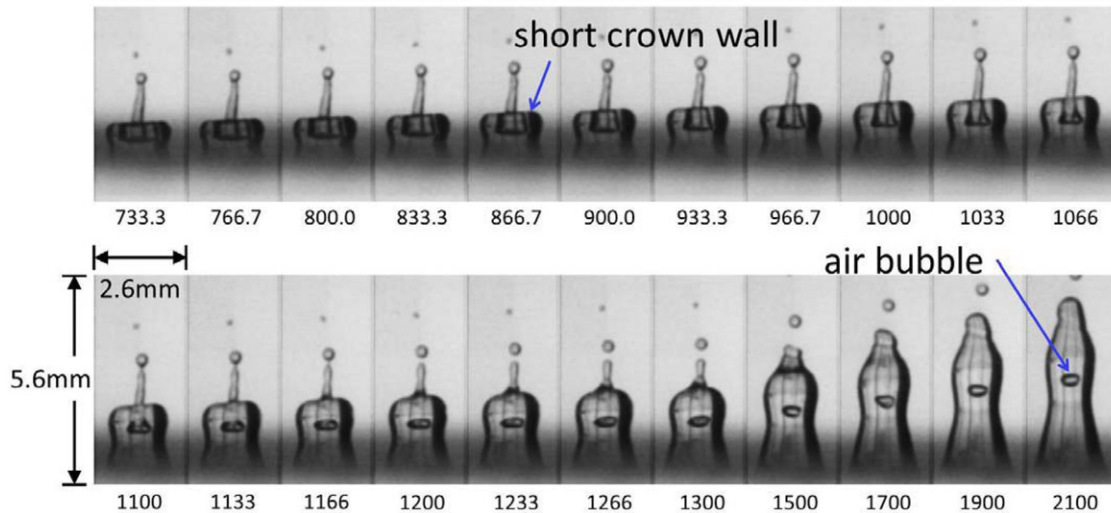
**Figure 5.** A typical result for morphological variations in the temporal evolution of the water jet generated at a depth of $\gamma = 1.04$. The frame rate is 30 kHz and the time (in $\mu$s) is indicated at the bottom of each frame.
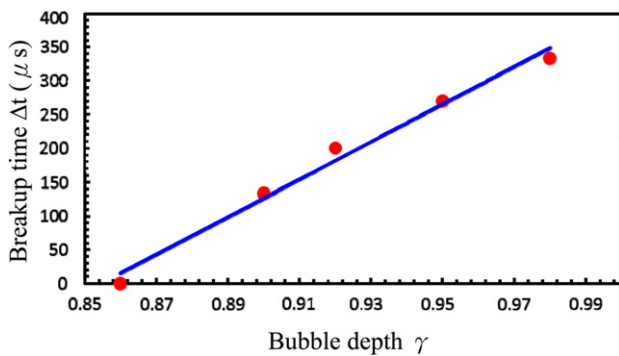


**Figure 6.** Experimental result for the time difference $\Delta t$ in the range $0.8 \leq \gamma \leq 1.03$.
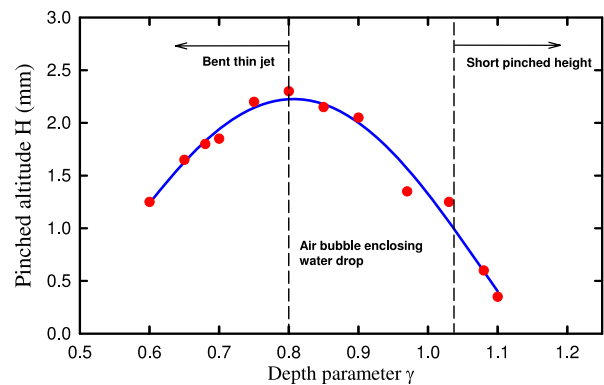


**Figure 7.** Dependence of the pinched altitude $H$ of the crown-shaped water jet on the depth parameter $\gamma$ in the range 0.6–1.1.

water jet on the depth parameter $\gamma$ is shown in figure 7. The solid line is a guide for the eye. Note that there is no crown-shaped water jet to be generated for $\gamma < 0.6$ or $\gamma > 1.1$. It can be seen that the highest pinched altitude occurs near the region of $\gamma = 0.8$ and its value is approximately 2.3 mm. For depth in the range $0.8 < \gamma < 1.1$, the decrease of the pinched altitude $H$ arises from the reduction of the interaction between the cavitation bubble and the free surface. The scope for the three types of morphological variation of the water jet in the temporal evolution is depicted in figure 7. In brief, a straight thin jet with a sufficient pinched altitude is necessary for the formation of an air bubble enclosing a water drop.

## 4. Conclusions

We have employed laser-induced water breakdown beneath a free flat surface to generate the structure of a thin water jet with a crown-shaped jet. With thorough investigations, morphological changes of the water jet in the temporal evolution can be divided into three regions depending on the depth parameter $\gamma$. In the first region with $0.6 < \gamma < 0.8$, the push force from the bubble on the free surface is so strong

that the thin jet is usually bending and inclines to the sidewall of the crown-shaped jet. In the second region with $0.8 \leq \gamma \leq 1.03$, the crown-shaped water jet is closing and finally forms an air bubble enclosing a water drop. In the last region with $1.03 < \gamma < 1.1$, the crown-shaped water jet cannot support a sufficient altitude and only an air bubble can be formed. This drop formation inside an air bubble is believed to provide more insight into the field of fluid dynamics.

## References

[1] Lauterborn W and Kurz T 2010 *Rep. Prog. Phys.* **73** 106501
[2] Benjamin T B and Ellis A T 1966 *Phil. Trans. R. Soc.* A **260** 221–40

[3] Philipp A and Lauterborn W 1998 *J. Fluid Mech.*
**361** 75–116

[4] Gaitan D F, Crum L A, Church C C and Roy R A 1992
*J. Acoust. Soc. Am.* **91** 3166–83

[5] Chahine G L 1977 *Trans. ASME* I **99** 709–15

[6] Blake J R and Gibson D C 1981 *J. Fluid Mech.* **111** 123–40

[7] Robinson P B, Blake J R, Kodama T, Shima A and Tomita Y
2001 *J. Appl. Phys.* **89** 8225–37

[8] Pearson A, Cox E, Blake J R and Otto S R 2004 *Eng. Anal.
Bound. Elem.* **28** 295–313

[9] Duocastella M, Patrascioiu A, Fernández-Pradas J M,
Morenza J L and Serra P 2010 *Opt. Express* **18** 21815–25

[10] Pain A, Goh B H T, Klaseboer E, Ohl S W and Khoo B C
2012 *J. Appl. Phys.* **111** 054912

[11] Chen R C C, Yu Y T, Su K W, Chen J F and Chen Y F 2013
*Opt. Express* **21** 445–53

[12] Obreschkow D, Kobel P, Dorsaz N, de Bosset A, Nicollier C
and Farhat M 2006 *Phys. Rev. Lett.* **97** 094502

[13] Robert E, Lettry J, Farhat M, Monkewitz P A and Avellan F
2007 *Phys. Fluids* **19** 067106

[14] Koita T, Zhu Y and Sun M 2011 *49th AIAA Aerospace
Sciences Meeting (4–7 Jan. 2011, Orlando)*
AIAA-2011-187

[15] Yamamoto H, Takayama K and Ishikawa K 2008 *J. Mineral.
Petrol. Sci.* **103** 192–203

[16] Tominaga T and Nakagawa A 2006 *Shock Waves* **15** 55–67

[17] Plateau J A F 1873 *Statique Expérimentale et Théorique des
Liquides Soumis aux Seules Forces Moléculaires* (Paris:
Gauthier-Villars)

[18] Rayleigh L 1879 *Proc. R. Soc. Lond.* **29** 71–97

[19] Yarin A L 2006 *Annu. Rev. Fluid Mech.* **38** 159–92

[20] Apitz I and Vogel A 2005 *Appl. Phys.* A **81** 329–38

[21] Lee M, Longoria R G and Wilson D E 1997 *Phys. Fluids*
**9** 540–50

[22] Mader C L and Gittings M L 2003 *Sci. Tsunami Hazards*
**21** 91–102

[23] Eggers J and Villermaux E 2008 *Rep. Prog. Phys.* **71** 036601